Int. J. Electrochem. Sci., 12 **(2017)** 5836 – 5844, doi: 10.20964/2017.07.01

International Journal of
ELECTROCHEMICAL
SCIENCE
www.electrochemsci.org

Facile Fabrication and Low-cost Coating of $LiNi_{0.8}Co_{0.15}Al_{0.05}O_2$ with Enhanced Electrochemical Performance as Cathode Materials for Lithium-ion Batteries

Huan Qi, Kui Liang[*]*, Wenxun Guo, Lingyun Tian, Xiaofeng Wen, Kaiyue Shi, Jusheng Zheng*

College of Materials Science and Engineering, Hunan University, Changsha 410082, China.
[*]E-mail: liangkui363@163.com

Received: 18 March 2017 / *Accepted:* 21 March 2017 / *Published:* 12 June 2017

The electrochemical performance of $LiNi_{0.8}Co_{0.15}Al_{0.05}O_2$ (NCA) was improved by coating with lithium boron oxide (LBO) via an effective, simple and low-cost method, where H_3BO_3 reacts with residual Li_2CO_3/LiOH on the surface of NCA to form LBO. LBO-coated NCA (LBO-NCA) had a better cycling stability and rate capability than bare NCA. After 50 cycles at 1C rate, 95.1% of the discharge capacity of LBO-NCA was retained, corresponding to 155 mAh g^{-1}, whereas bare NCA showed a discharge capacity retention of only 84.5%. In addition, LBO-NCA showed a discharge specific capacity of 153 mAh g^{-1} and 140 mAh g^{-1} at 2C and 5C, respectively, compared with bare NCA, which showed 145 mAh g^{-1} and 128 mAh g^{-1}. The improvement in the rate capability of LBO-NCA is mainly attributed to the LBO coating layer greatly decreasing the charge-transfer resistance.

Keywords: H_3BO_3; coating; facile; low cost; $LiNi_{0.8}Co_{0.15}Al_{0.05}O_2$

1. INTRODUCTION

Recently, much effort has been devoted to developing advanced cathode materials based on $LiNi_xCo_yM_{1-x-y}O_2$ (M=Mn, Al) due to their high capacity, low cost, and extended life cycle [1,2]. Among these cathode materials, NCA is regarded as one of the most promising owing to its intrinsic characteristics, such as good thermal stability and high capacity [3]. However, the cycling stability and rate capability of NCA are not high enough to meet application requirements, and thus, further improvements are needed. It has been proven that the presence of CO_2/H_2O in air and the spontaneous redox reaction of Ni^{3+} to Ni^{2+} can promote the formation of residual Li_2CO_3/LiOH on the surface of NCA materials. Furthermore, with an increase in the Ni content, the residual Li_2CO_3/LiOH and the degree of Li/Ni cation mixing on the surface of NCA materials increase, leading to severe safety issues and poor cycle life [4-13].

Among the many methods developed by researchers to solve these problems, surface coating is regarded as an effective way to improve the cycling stability and rate capability of NCA materials. Metal oxides, such as Nb_2O_5, Ta_2O_5 and ZrO_2 [14], are used as electrochemically inactive coating layers to decrease the electrode/electrolyte interface reaction and improve the cycle stability. However, a common drawback of these coatings is their low ionic conductivity, which is harmful to the rate capability. Meanwhile, electrochemically active materials, such as $LiCoO_2$ [4], Li_2ZrO_3 [15] and $Li_4Ti_5O_{12}$ [16], can also act as coating layers to improve the migration of Li^+. Lim [17] and Wang [18] have prepared Li_2O-$2B_2O_3$ coating layers with boric acid and lithium hydroxide; however, lithium hydroxide is expensive and harmful to the environment.

In this article, a facile and low-cost method was adopted to modify the surface structure of NCA materials with H_3BO_3, which is inexpensive and environmentally friendly. H_3BO_3 has been employed as a flux and network former for ceramics due to its good wetting properties and relatively low viscosity. Thus, H_3BO_3 was applied to NCA materials to react with residual Li_2CO_3/LiOH on the surface of NCA to form a LBO coating layer [19], which is electrochemically active and has high ionic conductivity. Here, the effects of the LBO coating with H_3BO_3 on the microstructure and electrochemical performance of NCA are reported.

2. EXPERIMENTAL

NCA powders were prepared as follows. The $[Ni_{0.8}Co_{0.15}Al_{0.05}](OH)_2$ precursor was synthesized by a co-precipitation method. An aqueous solution of $NiSO_4{\cdot}6H_2O$, $CoSO_4{\cdot}7H_2O$, and $Al(NO_3)_3{\cdot}9H_2O$ (molar ratio Ni:Co:Al=80:15:5) was added to a four-necked round-bottom flask under N_2 atmosphere. Meanwhile, a NaOH solution with a set amount of NH_4OH was added into the flask and stirred for 18 h at 45 ℃. Then, the slurry was dried in air at 80 ℃ overnight. NCA was prepared by heating the precursor homogenously mixed with $LiOH{\cdot}H_2O$ (1:1.05 molar ratio) at 800 ℃ for 15 h under oxygen flow. The LBO-coated NCA sample, denoted LBO-NCA, was prepared by the molten salt method. H_3BO_3 was completely dissolved in ethyl alcohol, and then, bare NCA powders were added into the solution under vigorous stirring. After evaporating the solvent at 80 ℃ for 4 h, the obtained powders were calcined at 500 ℃ for 10 h. Finally, the LBO-NCA powders were obtained after the mixture was cooled to room temperature.

Powder X-ray diffraction employing Cu-Kα radiation was used to identify the crystalline phase of the prepared powder at each stage. XRD data were obtained over 2θ=10-80 °, with a step size of 0.02 and a count time of 0.15 s. In addition, the morphology of the powders was observed by scanning electron microscopy and transmission electron microscopy.

To evaluate the electrochemical performance of the cathode materials, 2032-type coin cells were assembled in an argon-filled glovebox. The positive electrode consisted of the active material, acetylene black, and polyvinylidene fluoride in a weight ratio of 80:10:10, and lithium foil was used as the negative electrode. A 1 M solution of $LiPF_6$ in ethylene carbonate (EC), dimethyl carbonate (DMC), and ethylene methyl carbonate (EMC) in a volume ratio of 1:1:1 was used as the electrolyte. The coin cells were tested for their initial charge and discharge capacity at a current density of 0.1C

(1C=200 mA g^{-1}), cycling stability at a current density of 1C for 50 cycles, and rate capability at a current density of 0.1-5C over a voltage range of 2.7-4.3 V. Cyclic voltammetry (CV) curves were collected between 3.0 and 4.5 V (vs. Li^+/Li) at a scan rate of 0.1 mV s^{-1}. Electrochemical impedance spectroscopy (EIS) was performed over a range of 100 kHz to 0.01 Hz.

3. RESULTS AND DISCUSSION

Fig. 1 shows the XRD patterns of bare NCA and LBO-NCA. Both diffraction patterns indicate the formation of a layered α-$NaFeO_2$-type structure, assuming a hexagonal structure in the R3m space group [17]. In addition, LBO-NCA has no additional peaks corresponding to impurities or secondary phases, compared with bare NCA, which implies that the LBO coating does not influence the crystal structure of NCA. As shown in Table 1, the I(003)/I(104) value of bare NCA is 1.15, which increases to 1.54 for LBO-NCA, indicating a decreasing degree of Li/Ni cation mixing [2]. As shown in Table 1, the lattice constants of LBO-NCA exhibit few changes compared with those of bare NCA, which indicates that the coating materials remained on the surface rather than incorporated into the host matrix.

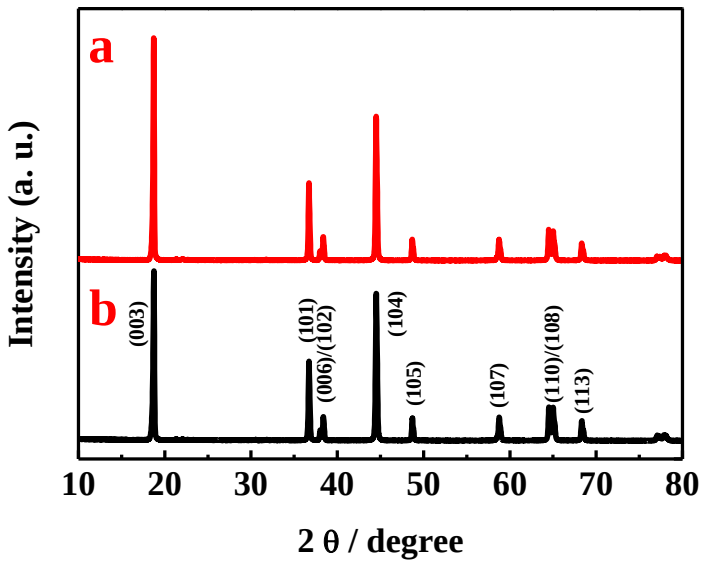

Figure 1. XRD patterns of (a) bare NCA and (b) LBO-NCA.

Table 1. Lattice parameters of bare NCA and LBO-NCA.

Sample	a (Å)	c (Å)	c/a	I(003)/I(104)
Bare NCA	2.86556	14.18472	4.94989	1.15
LBO-NCA	2.86607	14.19015	4.95108	1.54

Figs. 2a and b show the scanning electron microscopy (SEM) images of bare NCA and LBO-NCA, respectively. It was found that the particles are composed of many small grains with diameters of 500-800 nm and a high degree of crystallinity. Additionally, there are many gaps among the small

grains, which allows electrolyte to penetrate into the material to improve the utilization of the positive electrode material. The surface morphology of bare NCA and LBO-NCA is similar, because the LBO coating layer is very thin and evenly spread. The different surface structures of LBO-NCA and bare NCA are presented in Figs. 2c and d. It can be observed that the LBO coating layer is coated compactly on the surface of the LBO-NCA particles. In contrast, no extra phases appear on the surface of the bare NCA particles.

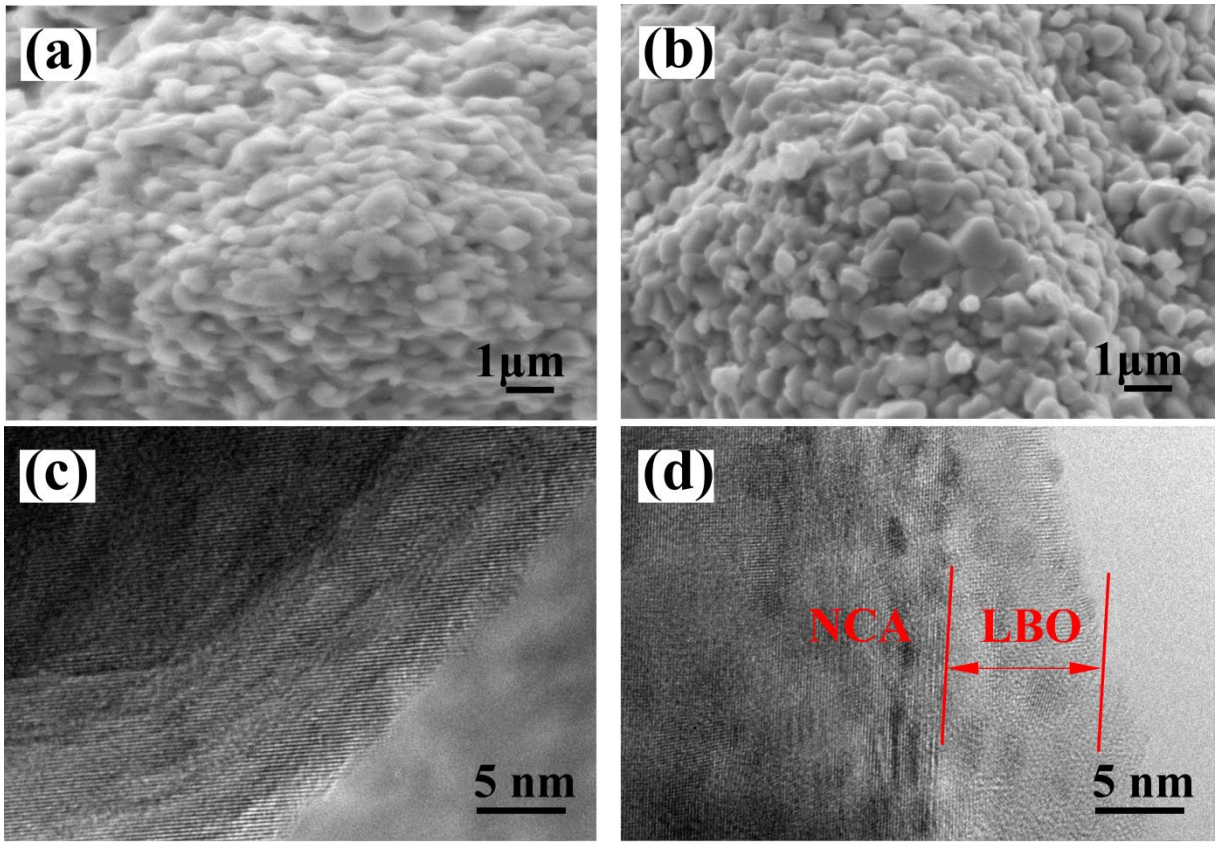

Figure 2. SEM images of (a) bare NCA and (b) LBO-NCA. TEM images of (c) bare NCA and (d) LBO-NCA.

Fig. 3a shows the initial charge-discharge curves of bare NCA and LBO-NCA over a voltage range of 2.7-4.3 V at a current density of 0.1C. Both charge-discharge profiles exhibit nearly the same potential plateaus. Bare NCA shows an initial discharge capacity of 189 mAh g^{-1} with a coulombic efficiency of 81.1%, and LBO-NCA delivers an initial capacity of 190 mAh g^{-1} with a coulombic efficiency of 84.4%. Both cells show similar initial discharge capacity, which indicates that the initial capacity is not affected by the LBO coating layer.

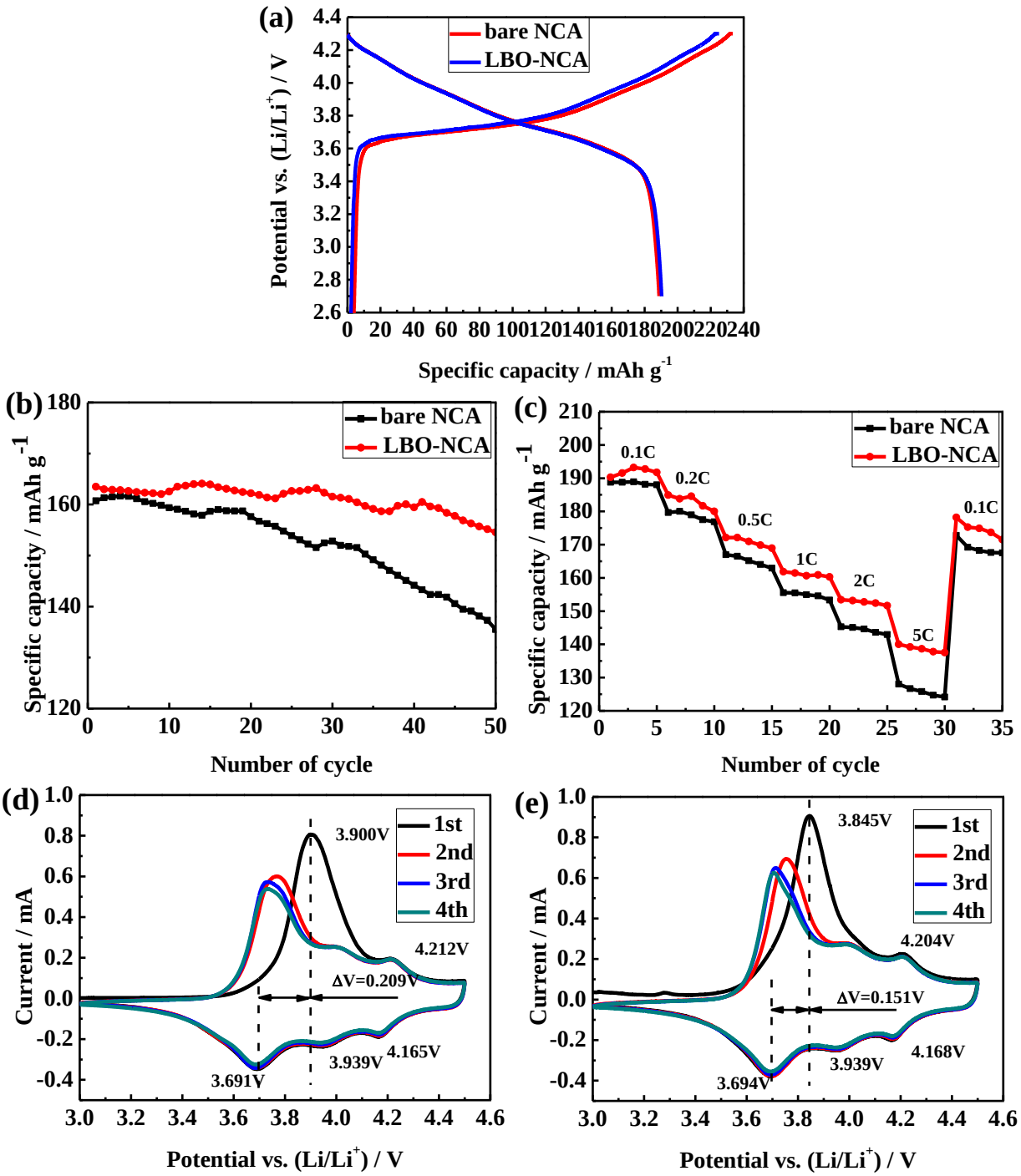

Figure 3. (a) Initial charge-discharge curves of bare NCA and LBO-NCA. (b) Cycling performances of bare NCA and LBO-NCA from 2.7 to 4.3 V. (c) Discharge capacity of bare NCA and LBO-NCA at various current densities. Cyclic voltammograms of (d) bare NCA and (e) LBO-NCA obtained at scan rate of 0.1 mV s^{-1}.

One of the critical performance parameters of Ni-rich cathode materials is the cycling stability. Poor capacity retention results from the structural instability of Ni-rich cathode materials, which causes the following processes: NiO formation accompanied by oxygen loss, dissolution of transition metal ions, and the production of harmful by-products from reactions between NCA and the electrolyte

[17]. Fig. 3b shows the cycling performance of NCA and LBO-NCA. Bare NCA and LBO-NCA show similar initial discharge capacities of 161 mAh g^{-1} and 163 mAh g^{-1} at 1C rate, respectively.

The LBO-NCA sample shows greatly improved capacity retention compared with bare NCA. For bare NCA, the discharge specific capacity is 136 mAh g^{-1} with a capacity retention of 84.5% after 50 cycles. Meanwhile, LBO-NCA shows a high discharge specific capacity of 155 mAh g^{-1} and high capacity retention of 95.1%. The improvement in the cycling stability is attributed to the formation of the LBO coating layer on the surface of NCA, which prevents the electrode surface from directly contacting the electrolyte, decreases the number of harmful by-products, and lessens the dissolution of transition metals from HF attacking the cathode surface [20-22].

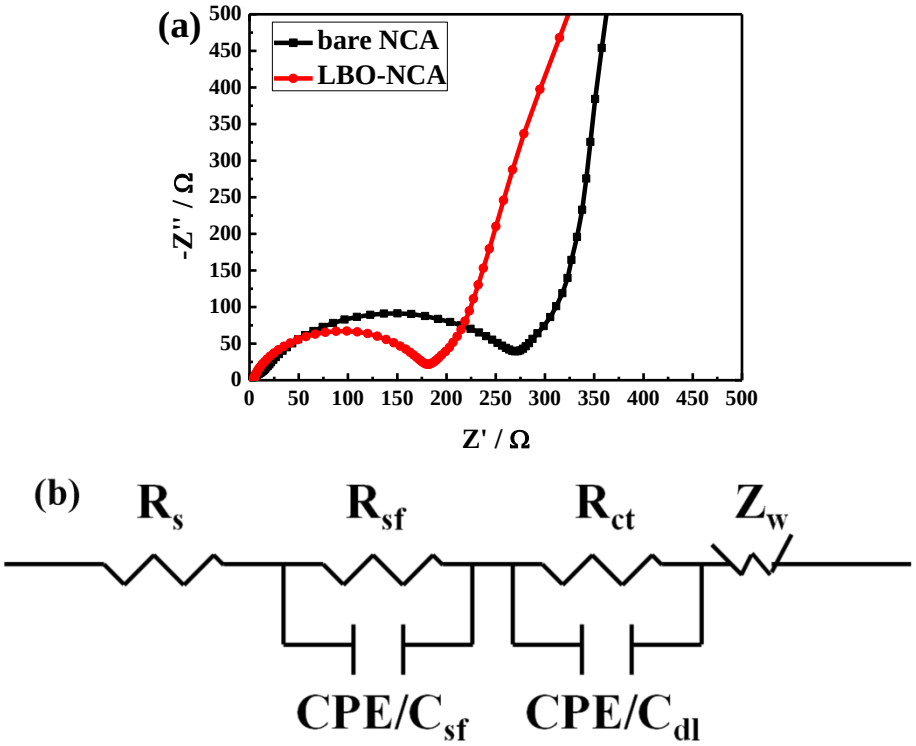

Figure 4. (a) Nyquist plots of bare NCA and LBO-NCA. (b) Equivalent circuit model used for fitting the EIS curves.

Fig. 3c shows the rate performance of bare NCA and LBO-NCA. Each cell was discharged at 0.1C, 0.2C, 0.5C, 1C, 2C, 5C and 0.1C over a voltage range of 2.7-4.3 V. It can be observed in Fig. 3c that LBO-NCA presents higher discharge specific capacities of 153 mAh g^{-1} and 140 mAh g^{-1} at 2C and 5C than that of bare NCA of 145 mAh g^{-1} and 128 mAh g^{-1}, respectively. The improvement in the rate capability of LBO-NCA is mainly attributed to the LBO coating layer, which decreases the charge-transfer resistance [23]. To elucidate the effect of the LBO coating on the electrochemical performance, comparisons between the LBO coating and other coating materials are given in Table 2. It can be observed that the LBO coating is superior to the other coatings.

Figs. 3d and e present the CV curves of bare NCA and LBO-NCA between 3.0 and 4.5 V (vs. Li^+/Li) at a scan rate of 0.1 mV s^{-1} over four cycles. For bare NCA (Fig. 3d), the anodic peaks in the first cycle were centered at 3.900 V and 4.212 V, corresponding to delithiation from the lattice. The cathodic peaks were centered at 4.165, 3.939, and 3.691 V, corresponding to intercalation of the Li ions. For LBO-NCA (Fig. 3e), the anodic peaks in the first cycle were centered at 3.845 and 4.204 V, and the cathodic peaks were centered at 4.168, 3.939, and 3.694 V. In the next three cycles, both samples displayed three anodic peaks and three cathodic peaks due to phase transitions from hexagonal to monoclinic (H1 to M), monoclinic to hexagonal (M to H2) and hexagonal to hexagonal (H2 to H3) during delithiation-lithiation [24,25]. As shown in Figs. 3d and e, the area under the cycle curve decreases with increasing cycles, which is consistent with the cycling performance. In addition, the difference in the first redox potential ΔV of bare NCA is 0.209 V, while that of LBO-NCA is 0.151 V. This indicates that the reversibility and reactivity of LBO-NCA were improved by the LBO coating.

Table 2. Comparison of the electrochemical performance of the LBO coating and other coating materials.

Coating materials on NCA	Initial discharge specific capacity		Cycle performance		Ref.
	Bare sample	Coated sample	Bare sample	Coated sample	
LBO (2.7-4.3 V, 25)	189 mAh g^{-1} (20 mA g^{-1})	190 mAh g^{-1} (20 mA g^{-1})	136/161 mAh g^{-1} ($50^{th}/1^{st}$ cycle, at 200 mAh g^{-1}, 84.5%)	155/163 mAh g^{-1} ($50^{th}/1^{st}$ cycle, at 200 mAh g^{-1}, 95.1%)	Our work
$LiCoO_2$ (2.8-4.3 V)	196.8 mAh g^{-1} (36 mA g^{-1})	196.2 mAh g^{-1} (36 mA g^{-1})	96.1% ($50^{th}/1^{st}$ cycle, at 36 mAh g^{-1})	98.7% ($50^{th}/1^{st}$ cycle, at 36 mAh g^{-1})	[3]
Vanadium-treated NCA (3.0-4.3 V)	198 mAh g^{-1} (21 mA g^{-1})	199 mAh g^{-1} (21 mA g^{-1})	78% ($200^{th}/1^{st}$ cycle, at 210 mAh g^{-1}, 60 ℃)	90% ($200^{th}/1^{st}$ cycle, at 210 mAh g^{-1}, 60 ℃)	[20]
CeO_2 (2.75-4.3 V)	181 mAh g^{-1} (40 mA g^{-1})	184 mAh g^{-1} (40 mA g^{-1})	78.2% ($100^{th}/1^{st}$ cycle, at 40 mAh g^{-1})	86% ($100^{th}/1^{st}$ cycle, at 40 mAh g^{-1})	[26]
SiO_2 (3-4.3 V, 60 ℃)	183 mAh g^{-1} (0.38 mA cm^{-2})	172 mAh g^{-1} (0.38 mA cm^{-2})	41/154 mAh g^{-1} ($40^{th}/1^{st}$ cycle, at 1.9 mA cm^{-2}, 27%)	98/160 mAh g^{-1} ($40^{th}/1^{st}$ cycle, at 1.9 mA cm^{-2}, 61%)	[27]

EIS is a useful technique for studying the kinetics of a cathode material. Lithium intercalation and deintercalation in a cathode material can be modelled as a multi-step process, which reflects the serial nature of several processes occurring during intercalation/deintercalation. The general nature of these models is to explain Li^+ migration through the surface film, charge-transfer through the electrode/electrolyte interface, and the solid-state diffusion of Li^+ in the compounds [18]. The impedance plots were fitted using the equivalent circuit model shown in Fig. 4b. The Nyquist plots of the cells assembled from bare NCA and LBO-NCA are shown in Fig. 4a. There is only one large semicircle present, which represents the charge-transfer resistance R_{ct}. The R_{ct} of LBO-NCA is smaller than that of NCA. The improved rate capability of LBO-NCA can be explained by the low charge-

transfer resistance at the interface between the electrode and electrolyte. Our experimental results reveal that the LBO layer can effectively protect NCA materials from contacting the electrolyte [28].

4. CONCLUSION

We synthesized LBO-coated NCA via an effective, simple and low-cost method, where H_3BO_3 reacts with residual Li_2CO_3/LiOH on the surface of NCA to form LBO. The initial specific capacity of LBO-NCA and bare NCA was similar, but the capacity retention was enhanced from 84.5% to 95.1% after coating with LBO. The specific capacity of LBO-NCA at 2C and 5C was higher than that of bare NCA. The improvement in the rate capability of LBO-NCA was mainly attributed to the LBO coating layer, which greatly decreased the charge-transfer resistance. Our results show that the LBO coating benefits the electrochemical performance of NCA, and our facile synthetic method could be adopted for large-scale production.

ACKNOWLEDGEMENTS
This work is supported by Jiang Su Oliter Energy Technology Co., Ltd.

References

1. C.H. Chen, J. Liu, M.E. Stoll, G. Henriksen, D.R. Vissers and K. Amine, *J. Power Sources*, 128 (2004) 278.
2. X. Li, Z.W. Xie, W.J. Liu, W.J. Ge, H. Wang and M.Z. Qu, *Electrochim~~i~~. Acta*, 174 (2015) 1122.
3. W.M. Liu, G.R. Hu, K. Du, Z.D. Peng and Y.B. Cao, *Surf. Coat. Technol*, 216 (2013) 267.
4. W.M. Liu, G.R. Hu, K. Du, Z.D. Peng and Y.B. Cao, *J. Power Sources*, 230 (2013) 201.
5. K. Masumoto, R. Kuzuo, K. Takeya and A. Yamanaka, *J. Power Sources*, 81-82 (1991) 558.
6. H.S. Liu, Z.R. Zhang, Z.L. Gong and Y. Yang, *Electrochem. Solid-State Lett.*, 7 (2004) A190.
7. G.V. Zhuang, G.Y. Chen, J. Shim, X.Y. Song, P.N. Ross and T.J. Richardson, *J. Power Sources*, 134 (2004) 293.
8. S.-W. Song, G.V. Zhuang and P.N. Ross, *J. Electrochem. Soc.*, 151 (2004) A1162.
9. H.S. Liu, Y. Yang and J.J. Zhang, *J. Power Sources*, 173 (2007) 556.
10. K. Shizuka, C. Kiyohara, K. Shima and Y. Takeda, *J. Power Sources*, 166 (2007) 233.
11. J. Eom, M.G. Kim and J. Cho, *J. Electrochem. Soc.*, 155 (2008) A239.
12. A.M. Andersson, D.P. Abraham, R. Haasch, S. MacLaren, J. Liu and K. Amine, *J. Electrochem. Soc.*, 149 (2002) A1358.
13. J. Kim, Y. Hong, K. S. Ryu, M. G. Kim and J. Cho, *Electrochem. Solid-State Lett.*, 9 (2006) A19.
14. S.-T. Myung, K. Izumi, S. Komaba, H. Yashiro, H.J. Bang, Y.-K. Sun and N. Kumagai, *J. Phys. Chem. C*, 111 (2007) 4061.
15. D. Wang, X.H. Li, W.L. Wang, Z.X. Wang, H.J. Guo and J.J Ru, *Ceramics International*, 41 (2015) 6663.
16. M. Sachs, M. Gellert, M. Chen, H.-J, Drescher, S.R. Kachel, H. Zhou, M. Zugermeier, M. Gorgoi, B. Rolinga and J. Gottfried, *Phys. Chem. Chem. Phys.*, 17 (2015) 31790.
17. S.N. Lim, W. Ahn, S.-H. Yeon and S.B. Park, *Electrochim. Acta*, 2014 (136) 1.
18. D. Wang, X.H. Li, Z.X. Wang, H.J. Guo, X. Chen, X.B. Zheng, Y. Xu and J.J. Ru, *Electrochim. Acta*, 174 (2015) 1225.

19. S.-H. Han, J.H. Song, T. Yim, Y.-J. Kim, J.-S. Yu and S. Yoon, *J. Electrochem. Soc.*, 163 (2016) A748.
20. M.-J. Lee, M. Noh, M.-H. Park, M. Jo, H. Kim, H. Nam and J. Cho, *J. Mater. Chem.* A, 3 (2015) 13453.
21. N.P.W. Pieczonka, Z.Y. Liu, P. Lu, K.L. Olson, J. Moote, B.R. Powell and J.-H. Kim, *J. Phys. Chem. C*, 117 (2013) 15947.
22. J. Cho and M.M. Thackeray, *J. Electrochem. Soc.*, 146 (1999) 3577.
23. J. Choi and A. Manthiram, *Solid State Ionics*, 176 (2005) 2251.
24. B. Huang, X.H. Li, Z.X. Wang, H.J. Guo and X.H. Xiong, *Ceramics International*, 40 (2014) 13223.
25. W. Li, J.N. Reimers and J.R. Dahn, *Solid State Ion.*, 67 (1993) 123.
26. S. Xia, Y. Zhang, P. Dong and Y. Zhang, *Eur. Phys. J. Appl. Phys.*, 66 (2014) 30403.
27. Y. Cho and J. Cho, *J. Electrochem. Soc.*,157 (2010) A625.
28. K. Du, J.L. Huang, Y.B. Cao, Z.D. Peng and G.R. Hu, *J. Alloy Compd.*, 574 (2013) 377.

© 2017 The Authors. Published by ESG (www.electrochemsci.org). This article is an open access article distributed under the terms and conditions of the Creative Commons Attribution license (http://creativecommons.org/licenses/by/4.0/).